# Defect types and room temperature ferromagnetism in N-doped rutile $TiO_2$ single crystals*

Qin Xiu-Bo(秦秀波)[a)d)†], Li Dong-Xiang(李东翔)[b)], Li Rui-Qin(李瑞琴)[b)], Zhang Peng(张 鹏)[a)], Li Yu-Xiao(李玉晓)[c)], and Wang Bao-Yi(王宝义)[a)]

[a)] *Key Laboratory of Nuclear Analysis Techniques, Institute of High Energy Physics, Chinese Academy of Sciences, Beijing* 100049, *China*
[b)] *School of Mathematics and Physics, Anshun University, Anshun* 561000, *China*
[c)] *School of Physical Engineering, Zhengzhou University, Zhengzhou* 450001, *China*
[d)] *Division for Nuclear Technology and Application, Institute of High Energy Physics, Chinese Academy of Sciences, Beijing* 100049, *China*

(Received 29 July 2013; revised manuscript received 3 December 2013; published online 10 April 2014)

The magnetic properties and defect types of virgin and N-doped $TiO_2$ single crystals are probed by superconducting quantum interference device (SQUID), X-ray photoelectron spectroscopy (XPS), and positron annihilation analysis (PAS). Upon N doping, a twofold enhancement of the saturation magnetization is observed. Apparently, this enhancement is not related to an increase in oxygen vacancy, rather to unpaired 3d electrons in $Ti^{3+}$, arising from titanium vacancies and the replacement of O with N atoms in the rutile structure. The production of titanium vacancies can enhance the room temperature ferromagnetism (RTFM), and substitution of O with N is the onset of ferromagnetism by inducing relatively strong ferromagnetic ordering.

**Keywords:** N doping, titanium vacancies, replacement of O with N atoms, ferromagnetism

**PACS:** 75.50.Pp, 71.55.–I, 75.20.Hr **DOI:** 10.1088/1674-1056/23/6/067502

## 1. Introduction

Dilute magnetic semiconductors (DMSs) have aroused much interest due to their favorable magnetic, magneto–optical, and magneto–electrical properties for application of spin-dependent electronic devices.[1] In the past decade, magnetic element doping has suffered from problems of cluster, precipitates or secondary phase formation, and the origin of ferromagnetism in the magnetic-transition-element-doped oxide semiconductor has been under debate. Recently, some research groups found that nonmagnetic ion-doped oxide semiconductors also exhibit ferromagnetism, namely, so-called "$d^0$" ferromagnetism.[2] Light elements such as C- and N-doped oxide semiconductors have aroused wide interest[3–5] since the nonmagnetic element doping may avoid the possible extrinsic ferromagnetism induced from the clustering of magnetic ions, precipitation or the formation of secondary phases.[6–8] The N-doped oxide semiconductor, ZnO, is first used as host and studied, both experimentally and theoretically. Subsequently, many theoretical studies based on first principles calculations were carried out to explore the ferromagnetisms of N-doped oxide semiconductors, such as N-doped $SnO_2$, $In_2O_3$, and $TiO_2$.[9–12] However, among these various N-doped $TiO_2$ semiconductors, few experimental results have been reported to confirm the predictions from these theoretical studies.

In this study, we show the effect of N-doping on the magnetic properties and defect types of $TiO_2$ rutile single crystals. Upon N-doping an enhancement of ferromagnetic ordering in terms of remanent and saturation magnetization is achieved. By combining X-ray diffraction (XRD), X-ray photoelectron spectroscopy (XPS), positron annihilation analysis (PAS), and superconducting quantum interference device (SQUID), we are able to show that with respect to the virgin sample, N doping can add saturation magnetization by the replacement of O with N atoms and titanium vacancies in the rutile structure. The selection of $TiO_2$ single crystals instead of thin films is expected to exclude any effect of possible magnetic impurities in the underlying substrates[13] and of the interfaces between films and substrates.[14]

## 2. Experiment

Commercial rutile $TiO_2$ single crystals were obtained from the Institute of Shanghai Optics and Fine Mechanics, Chinese Academy of Sciences. The size of the samples was 5 mm×5 mm×0.5 mm, corresponding to 53.25 mg in mass. The nitrogen implantation was performed at an energy of 160 keV in a vacuum chamber of $2\times10^{-3}$ Pa, with the nominal dose varying from $1\times10^{16}$ ions/cm$^2$ to $1\times10^{17}$ ions/cm$^2$ to $1\times10^{18}$ ions/cm$^2$. The samples thereafter were named 1E16, 1E17, and 1E18. XRD and XPS were used for the crystal

*Project supported by the Young Scientists Fund of the National Natural Science Foundation of China (Grant No. 61006066).
†Corresponding author. E-mail: qinxb@ihep.ac.cn
© 2014 Chinese Physical Society and IOP Publishing Ltd 

characterization and phase analysis. Magnetic properties of all samples were evaluated by using a highly sensitive SQUID (MPMS XL-5). PAS was also carried out for the evaluation of defects at room temperature with a monoenergetic positron beam. The energy of the positrons could be continuously adjusted in a range of 0 keV–20 keV, and about $4\times10^5$ counts were accumulated per given energy.

## 3. Results and discussion

First, we use XRD to characterize the phases of N-doped $TiO_2$ single crystals. XRD analyses show that all the samples have only rutile structures, and no impurity phases are detected within the detection limit of the instrument. One representative XRD spectrum is shown in Fig. 1 for the $1\times10^{18}$ nitrogen ion/cm implanted sample.

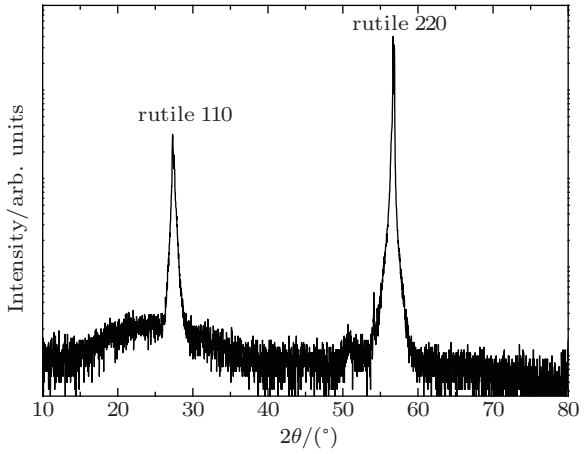



**Fig. 1.** XRD spectrum of $1\times10^{18}$ nitrogen ions /cm$^2$ implanted sample.

Figure 2(a) shows the *M*–*H* loops measured at 300 K for virgin and N-implanted $TiO_2$ single crystals with dose values of $1\times10^{16}$ ions/cm$^2$ to $1\times10^{17}$ ions/cm$^2$ to $1\times10^{18}$ ions/cm$^2$ respectively. All substrates display diamagnetic behavior[15] that is different from that of Zhou *et al* (paramagnetic).[16] The diamagnetism and ferromagnetism are proportional to magnetic field in N-doped samples. Figure 2(b) shows the N doping-fluence-dependent magnetization of $TiO_2$ single crystals after subtracting the diamagnetic background. The magnetic moment increases gradually with the increase of doping dose, but for the implanted dose with $1\times10^{18}$ ions/cm$^2$ it decreases significantly. We also measure the hysteresis loops at different doping doses. The loops are weakly doping-dose-dependent.

The effects of N on the electronic properties of the doped samples are discussed by examining the Ti 2p and N 1s core level X-ray photoelectron spectroscopy spectra. Figure 3 shows the Ti 2p XPS spectra obtained from the virgin $TiO_2$ single crystal and from the N-doped single crystals. These spectra are fitted by three Gaussians. The Ti 2p spectra show the typical spin–orbit split doublet of the $Ti^{4+}$ ion at binding energy BE = 458.4 eV and BE = 464.2 eV respectively. Unlike other samples, the sample 1E16 has both $Ti^{4+}$ ions and $Ti^{3+}$ ions. When the lattice oxygen is removed (due to the N irradiation) from rutile structure, the excess electrons which turn unpaired,[17] tend to occupy the nearby localized Ti 3d orbit and convert $Ti^{4+}$ ions into $Ti^{3+}$ ions. Then with the increase of the N doping dose, excess N ions could fill oxygen vacancies, which leads to the conversion of $Ti^{3+}$ ions into $Ti^{4+}$ ions. Some studies[16] elucidated that $Ti^{3+}$ ions with one unpaired 3d electron provide the local magnetic moments, but we also found the hysteresis loops in sample 1E17 and sample 1E18 by SQUID magnetometry, which indicate that the unpaired 3d electrons are not the main reason for the existence of room temperature ferromagnetism (RTFM) in N-doped $TiO_2$ single crystals.

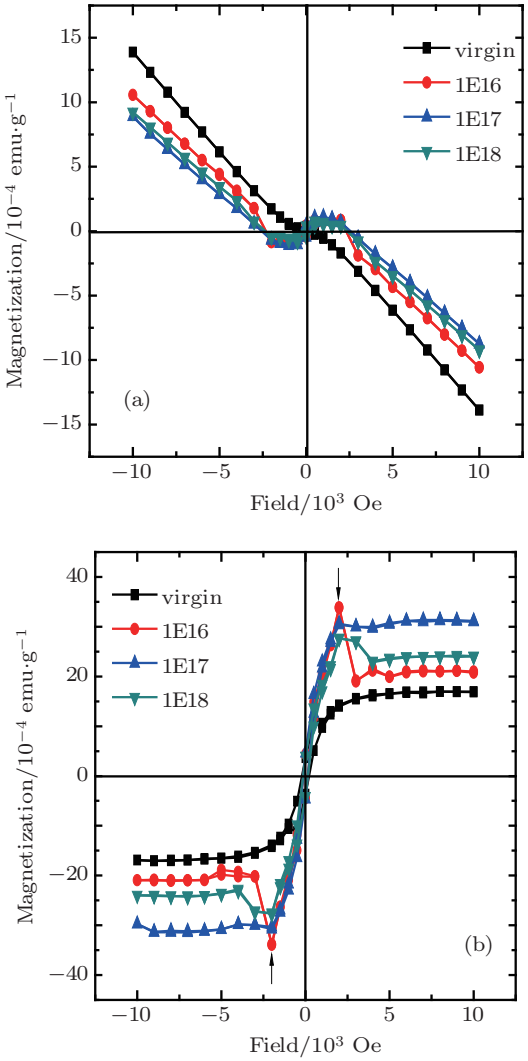



**Fig. 2.** (color online) (a) Original *M*–*H* curves of virgin and N-doped $TiO_2$ single crystals at 300 K, with the dose values being $1\times10^{16}$, $1\times10^{17}$, and $1\times10^{18}$ ions/cm$^2$ respectively. (b) *M*–*H* curves after subtracting the substrate signal. The anomalous protrusions in the curves are marked by arrows. The unit 1 Oe = 79.5775 A·m$^{-1}$.

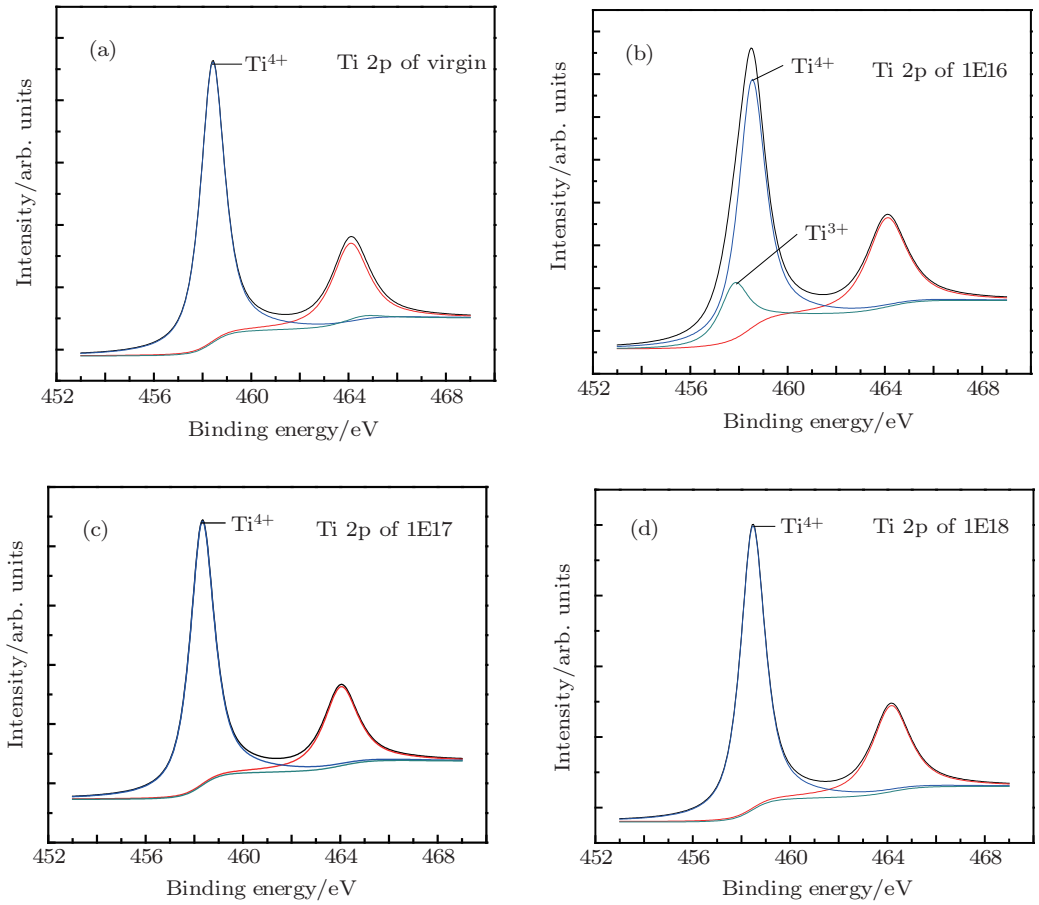



**Fig. 3.** (color online) Ti 2p XPS spectra for (a) virgin $TiO_2$ and N-doped $TiO_2$ with the dose values of (b) $1\times10^{16}$, (c) $1\times10^{17}$, and (d) $1\times10^{18}$ ions/cm$^2$.

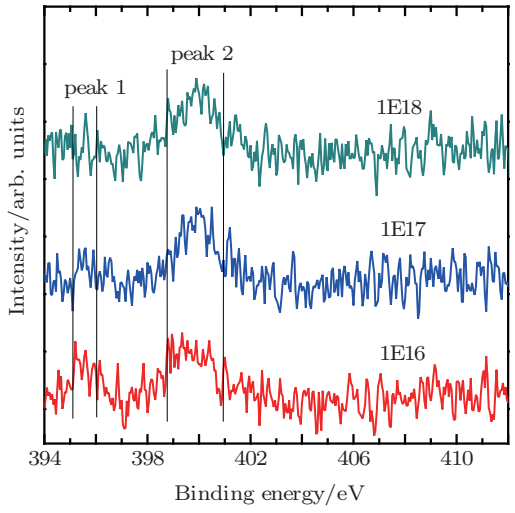



**Fig. 4.** (color online) N 1s spectra for N-doped $TiO_2$ samples with the dose values of $1\times10^{16}$ ions/cm$^2$, $1\times10^{17}$ ions/cm$^2$ to $1\times10^{18}$ ions/cm$^2$.

Figure 4 shows N 1s spectra for N-doped $TiO_2$ with the different doping doses. N-doped samples each show that two peaks appear at 395 eV–396.2 eV and 399 eV–401 eV respectively. It is known that N in $TiO_2$ has several states, such as interstitial (396 eV–397 eV), TiN state (396 eV–397 eV), and substitution Ti–O–N ($\sim$ 400 eV). Therefore, the N ions exist due to the formation of Ti–O–N bond, interstitial occupation or Ti–N–N bond in doped single crystals.

To verify the scenario, positron annihilation spectroscopy (PAS) measurements are performed to detect cation vacancies. As is well known, PAS is very sensitive to negatively charged and neutral vacancy-type defects and has been proved to be a powerful tool to investigate vacancy defects in semiconductors.[18] With the help of PAS, the vacancy defects can be identified and their concentrations are determined. Figure 5(a) shows the plots of the $S$ parameter versus positron implantation energy for virgin $TiO_2$ and N-doped $TiO_2$ with the dose values of $1\times10^{16}$, $1\times10^{17}$, and $1\times10^{18}$ ions/cm$^2$. Figure 5(b) shows the plots of the $S$ value versus $W$ value for two types of samples. It can be seen that the $S$ and $W$ values lie on a straight line for virgin $TiO_2$ single crystal, which means a single annihilation mechanism. But for N-doped samples, two kinds of annihilation mechanisms can be found, and one of them at (0.0876, 0.4125) is believed to be induced by N implantation. As is well known, $V_{Ti}$-related defects are the main defect trapping positrons inside the $TiO_2$ crystals. By combining XPS measurement, the other annihilation mechanism may be $V_{Ti}$–$N_O$ complexes. Based on change of the $S$ shown in Fig. 5(a), the plots can be divided into three parts. In part I

in an energy range from 0 to 2.5 keV, the *S* decreases sharply with the increase of energy, which is due to the positron annihilations and formation of positronium atoms at the surface of the samples.[19] The plots in part II in an energy range between 2.5 keV and 12 keV can be regarded as the characteristics of virgin and doped samples. In part II, the *S* parameter of N-doped $TiO_2$ crystal shows a distinct increase in comparison with that of virgin crystal, implying that the number of defects ($V_{Ti}$ and $V_{Ti}$–$N_O$) increases with the increase of N doping concentration, and it reaches a maximum for the 1E18 sample. While in part III in an energy range of 12 keV–20 keV, positrons annihilate mainly in the substrate, leading to overlapping of the plots.

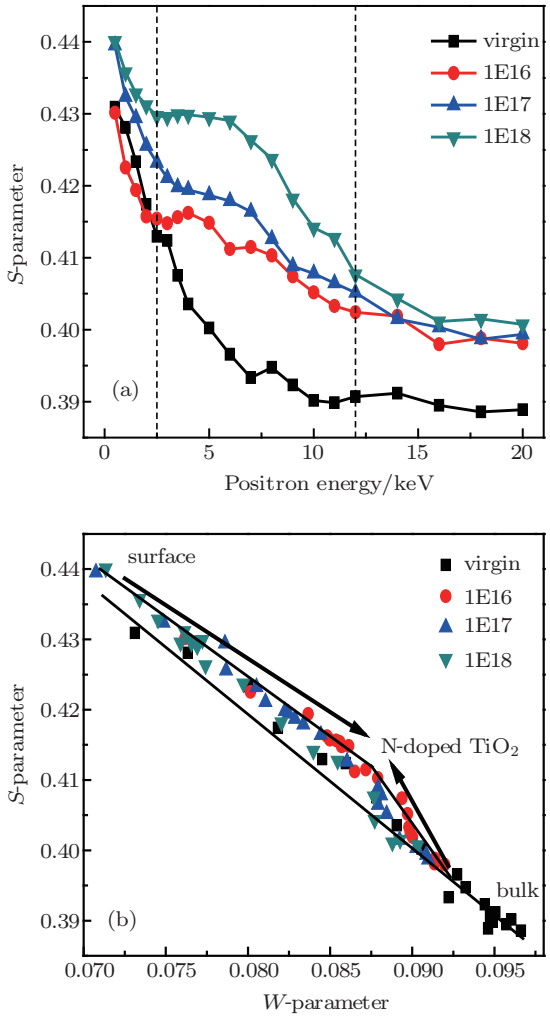



**Fig. 5.** (color online) (a) Variations of *S* values with incident positron energy (a) and with *W* value (b) for the samples: virgin $TiO_2$ and N-doped $TiO_2$ with the dose values of $1\times10^{16}$ ions/cm$^2$, $1\times10^{17}$ ions/cm$^2$ to $1\times10^{18}$ ions/cm$^2$ respectively.

Recently, the theoretical reports suggested that the ferromagnetism originates from the substitution of O with N. It is possible to activate ferromagnetism coupling between adjacent N dopants. Examination of spin density distribution and DOS spectra reveals that the p–p interaction between N and O is the origin of ferromagnetism coupling in this system. The hole-mediated double-exchange mechanism plays a major role in forming the ferromagnetism for N-doped $TiO_2$ system.[11] Our experimental measurements show that in the N-doped samples there exist mainly $V_O$, $V_{Ti}$, $N_O$, and $V_{Ti}$–$N_O$ defects. In the present work, the saturation magnetization of N-doped $TiO_2$ single crystals increases initially and then decreases as N concentration increases in the $1\times10^{18}$ ions/cm$^2$ dose. It can be explained as follows: when N doping concentration is low, a small number of $V_{Ti}$ and $N_O$ defects are induced in sample 1E16, leading to weak saturation magnetization. When further increasing N concentration, more $V_{Ti}$ and $N_O$ defects are generated in sample 1E17. However, for sample 1E18, excess N ions could fill oxygen vacancies due to the formation of $V_{Ti}$–$N_O$ complexes which make the saturation magnetization decrease. Moreover, the loops are weakly dependent on doping dose, indicated by SQUID measurement. Combining with XPS and PAS, it may clarify that the substitution of O can provide more favorable conditions for the onset of ferromagnetic ordering,[20] and the titanium vacancies can enhance the RTFM. Further, due to localized defect clusters, the RTFM may have localization.

## 4. Conclusion

Summarizing our results, we conclude the following. (i) A $V_{Ti}$–$N_O$ complex is generated due to ion irradiation. (ii) The saturation magnetization of N-doped $TiO_2$ single crystals increases with N doping dose increasing up to $1\times10^{16}$ ions/cm$^2$ and $1\times10^{17}$ ions/cm$^2$, but decreases at $1\times10^{18}$ ions/cm$^2$ due to the formation of the $V_{Ti}$–$N_O$ complexes. The RTFM is attributed to $V_{Ti}$ and $N_O$ defects in the rutile structure. The production of titanium vacancies can enhance the RTFM, and substitution of O with N is the onset of ferromagnetism by inducing relatively strong ferromagnetic ordering.

## Acknowlegment

The authors would like to thank Rahman Abu Zayed for advice given.

## References

[1] Pearton S J, Heo W H, Ivill M 1, Norton D P and Steiner T 2004 *Semicond. Sci. Technol.* **19** R59
[2] Pammaraju C D and Sanvito S 2005 *Phys. Rev. Lett.* **94** 217205
[3] Zhang B Y, Yao B, Li Y F, Liu A M, Zhang Z Z, Li B H, Xing G Z, Wu T, Qin X B, Zhao D X, Shan C X and Shen D Z 2011 *Appl. Phys. Lett.* **99** 182503
[4] Li W Q, Cao J X, Ding G W and Hu X D 2011 *J. Appl. Phys.* **110** 123908
[5] Bao N N, Fan H M, Ding J and Yi J B 2011 *J. Appl. Phys.* **109** 07C302
[6] Ney A, Ollefs K, Ye S, Kammermeier T, Ney V, Kaspar T C, Chambers S A, Wilhelm F and Rogalev A 2008 *Phys. Rev. Lett.* **100** 157201

[7] Kaspar T C, Droubay T, Heald S M, Nachimuthu P, Wang C M, Shutthanandan V, Johnson C A, Gamelin D R and Chambers S A 2008 *New J. Phys.* **10** 055010
[8] Yi J B, Lim C C, Xing G Z, Fan H M, Van L H, Huang S L, Yang K S, Huang X L, Qin X B, Wang B Y, Wu T, Wang L, Zhang H T, Gao X Y, Liu T, Wee A T S, Feng Y P and Ding J 2010 *Phys. Rev. Lett.* **104** 137201
[9] Long R and English N J 2009 *Phys. Lett. A* **374** 319
[10] Guan L X, Tao J G, Huan C H A, Kuo J L and Wang L 2009 *Appl. Phys. Lett.* **95** 012509
[11] Tao J G, Guan L X, Pan G S, Huan C H A, Wang L, Kuo J L, Zhang Z, Chai J W and Wang S J 2009 *Appl. Phys. Lett.* **95** 062505
[12] Wang H X, Zong Z C, Yan Yu and Qi S W 2012 *J. Magn. Magn. Mater.* **324** 2858
[13] Golmar F, Mudarra Navarro A M, Rodíguez Torres C E, Sánchez F H, Saccone F D, dos Santos Claro P C, Benítez G A and Schilardi P L 2008 *Appl. Phys. Lett.* **92** 262503
[14] Brinkman A, Huijben M, van Zalk M, Huijben J, Zeitler U, Maan J C, van der Wiel W G, Rijnders G, Blank D H A and Hilgenkamp H 2007 *Nat. Mater.* **6** 493
[15] Liu C M, Xiang X, Zhang Y, Jiang Y and Zu X T 2011 *Chin. Phys. Lett.* **28** 127201
[16] Zhou S Q , Čižmár E, Potzger K, Krause M, Talut G, Helm M, Fassbender J, Zvyagin S A, Wosnitza J and Schmidt H 2009 *Phys. Rev. B* **79** 113201
[17] von Oertzen G U and Gerson A R 2007 *J. Phys. Chem. Solids* **68** 324
[18] Tuomisto F and Ranki V 2007 *Phys. Rev. B* **76** 165207
[19] Yang A L, Song H P, Liang D C, Wei H Y, Liu X L, Jin P, Qin X B, Yang S Y, Zhu Q S and Wang Z J 2010 *Appl. Phys. Lett.* **96** 151904
[20] Drera G, Mozzati M C, Galinetto P, Diaz-Fernandez Y, Malavasi L, Bondino F, Malvestuto M and Sangaletti L 2010 *Appl. Phys. Lett.* **97** 012506